ACCOUNTS of chemical research

Article

Cite This: Acc. Chem. Res. 2019, 52, 1289−1300

pubs.acs.org/accounts

Heterogenized Molecular Catalysts: Vibrational Sum-Frequency Spectroscopic, Electrochemical, and Theoretical Investigations

Aimin Ge,[†,∥] Benjamin Rudshteyn,[‡,∥] Pablo E. Videla,[‡,∥] Christopher J. Miller,[§] Clifford P. Kubiak,*[,§] Victor S. Batista,*[,‡,§] and Tianquan Lian*[,†]

[†]Department of Chemistry, Emory University, Atlanta, Georgia 30322, United States

[‡]Department of Chemistry and Energy Sciences Institute, Yale University, New Haven, Connecticut 06520, United States

[§]Department of Chemistry and Biochemistry, University of California, San Diego, 9500 Gilman Drive, MC 0358, La Jolla, California 92093, United States

CONSPECTUS: Rhenium and manganese bipyridyl tricarbonyl complexes have attracted intense interest for their promising applications in photocatalytic and electrocatalytic CO_2 reduction in both homogeneous and heterogenized systems. To date, there have been extensive studies on immobilizing Re catalysts on solid surfaces for higher catalytic efficiency, reduced catalyst loading, and convenient product separation. However, in order for the heterogenized molecular catalysts to achieve the combination of the best aspects of homogeneous and heterogeneous catalysts, it is essential to understand the fundamental physicochemical properties of such heterogeneous systems, such as surface-bound structures of Re/Mn catalysts, substrate−adsorbate interactions, and photoinduced or electric-field-induced effects on Re/Mn catalysts. For example, the surface may act to (un)block substrates, (un)trap charges, (de)stabilize particular intermediates (and thus affect scaling relations), and shift potentials in different directions, just as protein environments do. The close collaboration between the Lian, Batista, and Kubiak groups has resulted in an integrated approach to investigate how the semiconductor or metal surface affects the properties of the attached catalyst. Synthetic strategies to achieve stable and controlled attachment of Re/Mn molecular catalysts have been developed. Steady-state, time-resolved, and electrochemical vibrational sum-frequency generation (SFG) spectroscopic studies have provided insight into the effects of interfacial structures, ultrafast vibrational energy relaxation, and electric field on the Re/Mn catalysts, respectively. Various computational methods utilizing density functional theory (DFT) have been developed and applied to determine the molecular orientation by direct comparison to spectroscopy, unravel vibrational energy relaxation mechanisms, and quantify the interfacial electric field strength of the Re/Mn catalyst systems.

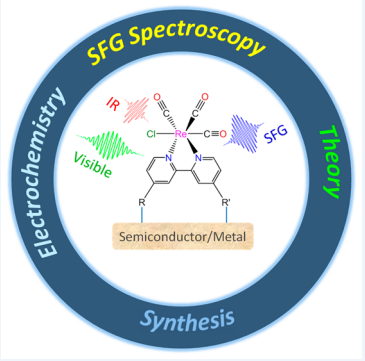

This Account starts with a discussion of the recent progress in determining the surface-bound structures of Re catalysts on semiconductor and Au surfaces by a combined vibrational SFG and DFT study. The effects of crystal facet, length of anchoring ligands, and doping of the semiconductor on the bound structures of Re catalysts and of the substrate itself are discussed. This is followed by a summary of the progress in understanding the vibrational relaxation (VR) dynamics of Re catalysts covalently adsorbed on semiconductor and metal surfaces. The VR processes of Re catalysts on TiO_2 films and TiO_2 single crystals and a Re catalyst tethered on Au, particularly the role of electron−hole pair (EHP)-induced coupling on the VR of the Re catalyst bound on Au, are discussed. The Account also summarizes recent studies in quantifying the electric field strength experienced by the catalytically active site of the Re/Mn catalyst bound on a Au electrode based on a combined electrochemical SFG and DFT study of the Stark tuning of the CO stretching modes of these catalysts. Finally, future research directions on surface-immobilized molecular catalyst systems are discussed.

1. INTRODUCTION

Molecular catalysts for CO_2 reduction have been extensively explored in recent years because of their potential application to reduce the atmospheric carbon footprint and provide sustainable alternative fuels.[1,2] In particular, rhenium bipyridyl tricarbonyl complexes have shown efficient and selective catalytic activities in the photocatalytic and electrocatalytic reduction of CO_2 to CO.[1,3−6] Re catalysts immobilized on solid surfaces have attracted increasing interest in recent years since they offer enhanced activity, reduced loading, and convenient product separation.[7−10] In such heterogenized systems, the electronic structure of the electrode and the strong electric field at the double layer play critical roles in affecting the adsorption configuration, energetics, and vibrational energy flow at interfaces, thus significantly affecting the reactivity and stability of adsorbed species. It is therefore of great interest to unravel the nature of the fundamental substrate−adsorbate interactions responsible for regulating catalytic mechanisms. Such an understanding would be particularly valuable for the development of molecular catalysts with higher activity, selectivity, and stability at interfaces.

Received: January 1, 2019
Published: May 6, 2019

DOI: 10.1021/acs.accounts.9b00001
Acc. Chem. Res. 2019, 52, 1289−1300

Because of the high sensitivity of the CO stretching modes to the solvation environment and electronic structure of the Re center,[11−13] surface-sensitive vibrational spectroscopic methods, such as attenuated total reflection infrared (ATR IR) and two-dimensional infrared spectroscopy, have been demonstrated to be powerful techniques for probing surface-immobilized molecular catalysts.[14−20] As an intrinsic surface-selective technique, vibrational sum-frequency generation (SFG) spectroscopy[21] offers an alternative robust spectroscopic approach with submonolayer sensitivity to investigate Re catalyst monolayers, providing information on the molecular orientation at various surfaces and interfaces.[22−26] Additionally, time-resolved SFG (TR-SFG) spectroscopy can probe ultrafast interfacial dynamics of the adsorbed catalysts, providing valuable information on the rates and mechanisms of energy and charge transfer at interfaces.[27−30] Complementing electrochemical measurements with in situ SFG spectroscopy can provide insight into redox reaction intermediates of the catalysts[31] as well as the effect of electric field on electrolyte−electrode interfaces.[25,32,33] Supplementing SFG measurements with computational methods offers insight into the bound structures of molecular catalysts and the mechanisms of vibrational energy relaxation and photo- and electrocatalytic reactions, providing a more complete molecular picture of the processes at the catalyst−substrate interfaces.

In this Account, we summarize recent experimental and theoretical studies of a family of heterogenized Re catalysts (Scheme 1), including catalysts on semiconductor and metallic surfaces. We show how various factors, including the crystal facet, length of the anchoring ligand, and doping levels in semiconductors influence the binding geometry of Re catalysts on various substrates, thus modulating the adsorbate−substrate interactions.[22−24,34−36] We further describe the effect of the anchoring group, crystalline structure of the TiO_2 substrate, and electron−hole pair coupling of Au surfaces on the vibrational energy relaxation of Re catalysts at interfaces, a fundamental process that plays an important role in controlling the vibrational energy transfer pathways, reactivity, and stability of intermediates.[27,28,30] Toward understanding the electrocatalytic mechanism, we also discuss the electric field strength experienced by the surface-bound Re catalyst and closely related Mn catalyst attached to Au electrodes by studying the Stark tuning of their CO stretching modes.[25]

Scheme 1. Rhenium Catalysts Examined in This Work

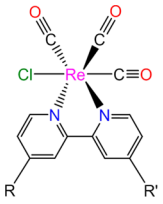

ReCnA	RediCN
R = R' = $(CH_2)_nCOO^-$	R = R' = CN
ReC1P	**ReS**
R = R' = $(CH_2)PO_3^{2-}$	R = S^- R' = H
ReCN	**ReC0-Au**
R = CN R'=H	R = R' = $COO-(CH_2)_{11}S^-$

2. VIBRATIONAL SFG SPECTROSCOPY

Since in the literature there exist many excellent reviews on SFG, here we present a brief introduction to the basic concepts of SFG and experimental setup implemented in Lian's group, referring the interested reader to more detailed references.[21,37,38] Vibrational SFG is a second-order nonlinear optical process in which a tunable IR laser beam with frequency ω_{IR} and a visible laser beam with frequency ω_{vis} are spatially and temporally overlapped at an interface to generate the SFG signal at frequency $\omega_{SFG} = \omega_{IR} + \omega_{vis}$ (Figure 1A). Because SFG is a second-order process, the SFG intensity is related to the second-order nonlinear susceptibility $\chi^{(2)}$ of the sample, which for an adsorbate on a surface can be modeled by a Lorentzian model:[39]

$$I_{SFG} \propto |\chi^{(2)}|^2 = \left| A_{NR} e^{i\phi} + \sum_n \frac{A_n}{\omega_{IR} - \omega_n + i\Gamma_n} \right|^2 \quad (1)$$

In the previous equation, A_n, ω_n, and Γ_n represent the amplitude, frequency, and line width (half width at half-maximum, HWHM) of the resonant nth vibrational mode of the adsorbate, whereas A_{NR} and ϕ represent the amplitude and phase of any nonresonant susceptibility. Under the electric dipole approximation, the SFG process is forbidden in media with inversion symmetry ($\chi^{(2)} = 0$) but is allowed in media where inversion symmetry is broken ($\chi^{(2)} \neq 0$). Therefore, SFG is ideal for probing the structure and dynamics of molecules at various surfaces and interfaces because of its intrinsic interface selectivity and submonolayer sensitivity. Moreover, because at the microscopic level the amplitude of the resonant nth vibrational mode A_n is related to the hyperpolarizability tensor of the molecule, β, which in turn depends on the absolute orientation of the molecule on the surface, comparison of the SFG intensities measured with different polarization combinations of the IR, visible, and SFG beams allows one to obtain orientational information.[21]

The femtosecond broadband SFG laser system used in Lian's group for the studies of heterogenized molecular catalysts is presented in Figure 1B. A Spitfire Ti:sapphire regenerative amplifier system produces 150 fs pulses at 800 nm (1 kHz, pulse energy 4 mJ). Half of the 800 nm output is used to make a narrowed-band beam (~10 cm^{-1}) by a pulse shaper. The other half of the 800 nm output is used to pump an optical parametric amplifier (TOPAS-C), producing tunable IR pulses with a bandwidth of ~200 cm^{-1}. Both pulses are focused on the surfaces of self-assembled monolayers (SAMs) of Re catalysts, which are prepared by overnight immersion of the semiconductor or metallic substrate in a stock solution of the catalyst. The reflected sum-frequency signal is collimated and refocused onto the slit of a 300 mm monochromator and detected with a liquid-nitrogen-cooled charge-coupled device (CCD) operating at −120 °C. The *ppp* polarization combination (*p* polarization for SFG, visible, and IR, as schematically shown in Figure 1B) is used for most measurements. To study the vibrational relaxation dynamics of molecular catalysts on substrates, TR-SFG can be used, where part of the IR output from the optical parametric amplifier is used as a pump beam (Figure 1B) to excite the catalyst. The pump IR beam is sent through a computer-controlled delay stage to control the timing of the IR pump pulse relative to the SFG probe pulse pair, and a chopper blocks every other pump pulse to produce pumped and unpumped SFG signals. The difference SFG spectrum obtained as the difference between the pump-on and pump-off signals is recorded as a function of delay time, and the kinetics is modeled to reveal the ultrafast population changes of the CO stretching modes.

DOI: 10.1021/acs.accounts.9b00001
Acc. Chem. Res. 2019, 52, 1289−1300

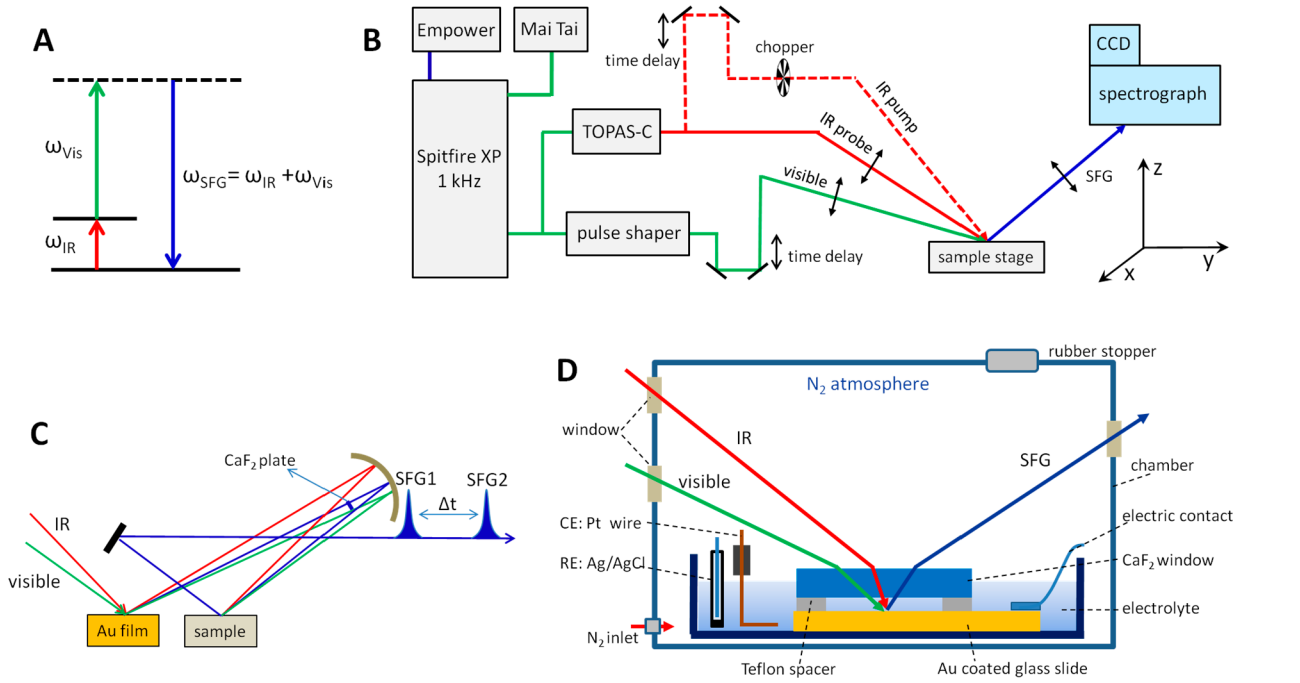

Figure 1. Experiemental setups for SFG measurements. (A) Energy level diagram of an SFG process. (B) Schematic of the femtosecond broadband SFG system implemented in Lian's group. A Spitfire Ti:sapphire regenerative amplifier produces 150 fs pulses at 800 nm (1 kHz, pulse energy 4 mJ). (C) Phase-sensitive SFG setup. (D) Sample chamber used for the electrochemical SFG measurements. (C) and (D) were adapted from refs 35 and 33, respectively. Copyright 2018 and 2017, respectively, American Chemical Society.

The total signal from conventional SFG measurements, given by eq 1, contains both the real and imaginary parts of the molecular responses and nonresonant contributions of the substrate as well as the cross terms of these signals, resulting in complex SFG signals that can be difficult to interpret. This complexity can be removed by phase-sensitive (heterodyne-detected) SFG (PS-SFG) measurements (Figure 1C) to obtain the imaginary part of the second-order susceptibility:[37]

$$\mathrm{Im}[\chi^{(2)}] = A_{\mathrm{NR}} \sin\phi + \sum_n \frac{-\Gamma_n A_n}{(\omega_{\mathrm{IR}} - \omega_n)^2 + \Gamma_n^2} \qquad (2)$$

PS-SFG measurements have two advantages over common SFG. First, the imaginary spectra obtained by phase-sensitive SFG avoid complicated interference between adjacent vibrational modes. Second, the nonresonant contribution generated from the substrate can be removed without relying on spectral fitting.[37] These features are beneficial for determining the binding geometry of surface-immobilized Re catalysts. The PS-SFG measurement is performed by interference of the SFG signal of a Re catalyst sample or a reference sample with the SFG signal of a bare gold film following published procedures (Figure 1C).[37]

Electrochemical SFG measurements of molecular catalysts immobilized on gold electrodes were carried out in a home-built chamber (Figure 1D).[33] A glass dish placed in the chamber was used as an electrochemical cell. The Au slide was attached by conducting copper tape and used as a working electrode. The copper tape was isolated from the electrolyte by epoxy resin. A 2 mm thick CaF_2 plate was used as the cell window and pressed on the surface of the Au slide. The distance between the CaF_2 window and Au surface was controlled by a 25 μm Teflon spacer. The plastic chamber was purged with nitrogen for ~15 min before the electrolyte solution (~10 mL) was injected into the electrochemical cell through a rubber stopper embedded in the plastic chamber. The plastic chamber was continuously purged with nitrogen during the SFG measurements.

3. INTERFACIAL STRUCTURES OF SURFACE-IMMOBILIZED RE CATALYSTS

When a molecular catalyst is immobilized on a surface, its efficiency and reaction pathways can be affected by particular adsorbate−substrate interactions that govern the interface electronic properties and the configuration of the catalytically active site.[6,8,40−43] Hence, understanding how the crystal facet and the nature of the anchoring ligands can affect the interfacial molecular geometry is of crucial importance to the design of efficient and robust molecular catalysts. By combining SFG spectroscopy and DFT calculations, we have elucidated interfacial structures of Re catalysts covalently attached to single-crystal semiconductors and metals, thus unraveling the effects of the substrate, crystal facet, anchoring group, and anchoring chain length on the binding geometry of the adsorbates.

3.1. Re Catalysts on TiO_2 Surfaces

Because of the atomically flat and well-characterized nature of crystalline TiO_2 surfaces as well as the importance of TiO_2 in electrocatalysis and photocatalysis applications,[8,44] Re catalysts self-assembled on single-crystalline TiO_2 surfaces offer an opportunity to investigate how the TiO_2 surface affects the binding geometry of the Re catalyst. Our first efforts were focused on characterizing the interfacial structure of Re(4,4′-dicarboxy-2,2′-bipyridine)$(CO)_3Cl$ (ReC0A), a Re catalyst with a simple carboxylate anchoring group, bound to a single-crystalline high-symmetry TiO_2 rutile surface.[34] Figure 2A shows the SFG spectra for three polarization combinations for ReC0A on the TiO_2(001) surface along with the Fourier transform infrared (FTIR) spectrum of ReC0A on nanoporous

DOI: 10.1021/acs.accounts.9b00001
Acc. Chem. Res. 2019, 52, 1289−1300

TiO_2. The FTIR spectrum is characterized by the three CO stretching modes (Scheme 2) typical of the Re metal carbonyl,

Scheme 2. Three Carbonyl Stretching Modes of the Re Catalysts (from Low to High Frequency): Out-of-Phase Symmetric Stretch, a′(2); Antisymmetric Stretch, a″; In-Phase Symmetric Stretch, a′(1)

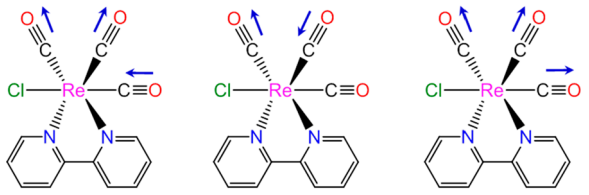

whereas in the SFG spectra only the symmetric stretching can be observed in certain polarizations, highlighting the orientational selectivity of SFG spectroscopy.[39] The azimuthal-angle-dependent SFG intensity, shown as a polar plot in Figure 2B, reveals that ReC0A molecules are isotropically arranged on the (001) surface, consistent with the C_4 symmetry of the (001) surface.[24] An orientational analysis based on the polarization dependence of the a′(1) mode peak intensity with the *ppp* and *sps* polarizations (I_{ppp}/I_{sps}) yields a tilt angle θ between the bipyridine ring and the surface normal of ∼0−22°. This orientation is confirmed by DFT calculations of a ReC0A molecule on a model TiO_2 slab, which predicts that both bidentate (Figure 2C) and tridentate (Figure 2D) binding modes can be found on the surface with tilt angles that lie within the experimental range. Since in the electrocatalytic cycle of Re complexes a key mechanistic step is reduction of the Re complex followed by loss of the Cl atom to form a Re^I species that can react with CO_2,[45] the vertical binding geometry of ReC0A on TiO_2(001) would leave the Re center atom well exposed to the solution and would be beneficial to obtain maximum reductive capacity of the catalyst.

To investigate how the nature of the anchoring group affects the orientation of the catalyst, we analyzed by PS-SFG spectroscopy (Figure 1C) a series of Re complexes with anchoring groups of various lengths ($Re(CnA)(CO)_3Cl$ [*C*nA = 2,2′-bipyridine-4,4′-$(CH_2)_n$COOH, n = 0−4]) immobilized on the TiO_2(001) surface.[22] Figure 3A shows the normalized experimental PS-SFG spectra of ReC*n*A. Although ReC0A exhibits only the a′(1) mode around ∼2040 cm^{-1} (consistent with the homodyne spectra shown in Figure 2A), all of other complexes also show an additional broad peak around ∼1900−1925 cm^{-1} assigned to the a′(2) and a″ modes. The significant difference in the SFG spectra of these complexes indicates that the methylene groups in the hydrocarbon linkers of ReC*n*A (n = 1−4) cause the orientation of ReC*n*A to deviating substantially from the normal orientation found for ReC0A on the rutile TiO_2(001) surface (Figure 2C,D). By combination of ab initio simulations of the PS-SFG spectra (Figure 3A) with a conformational search, the average molecular orientation of ReC*n*A on the TiO_2(001) surface was determined. We found that bipyridine ring of the Re complexes tilts progressively further toward the TiO_2(001) surface as the number of methylene groups increases (Figure 3B).[22] We anticipate that exposure of the Cl catalytically active site to the substrate CO_2 in solution should enhance catalysis while blocking of the CO_2 binding site by the surface likely suppresses the reactivity. These results demonstrate that the molecular orientation of Re catalysts covalently bound to semiconductor surfaces could be designed by tailoring the length of the anchoring groups, though one needs to consider the increased disorder when the anchoring groups are longer.

To explore the effect of the symmetry of the underlying substrate on the molecular arrangement of Re catalysts, we also

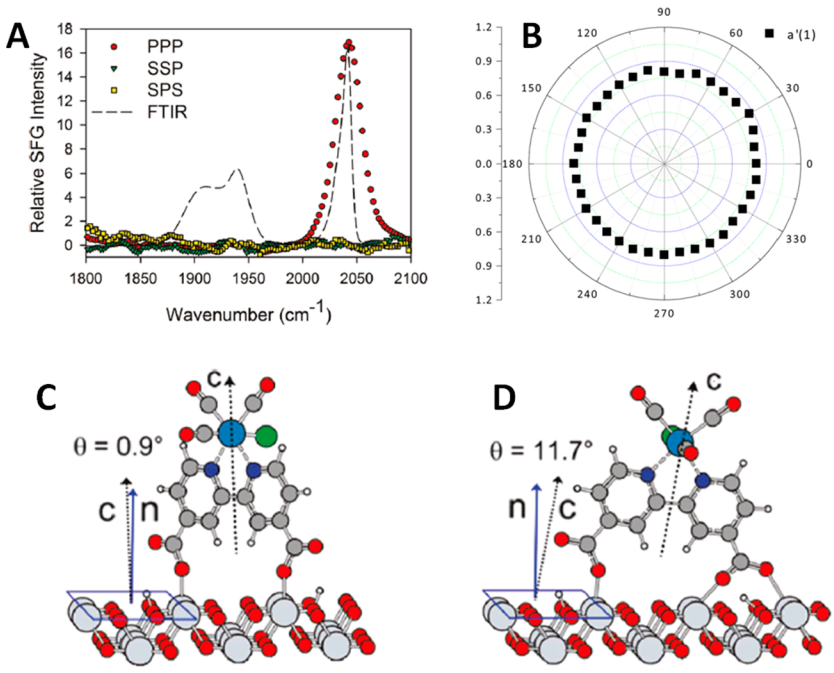

Figure 2. Combined SFG and DFT study of ReC0A on the rutile TiO_2(001) surface. (A) SFG spectra of three polarization combinations and the FTIR spectrum of ReC0A adsorbed on a TiO_2 thin film. (B) Polar plot of the experimental azimuthal dependence of the amplitude of the a′(1) mode. (C, D) Calculated adsorption geometries. Adapted from refs 34. and 24. Copyright 2011 and 2016, respectively, American Chemical Society.

DOI: 10.1021/acs.accounts.9b00001
Acc. Chem. Res. 2019, 52, 1289−1300

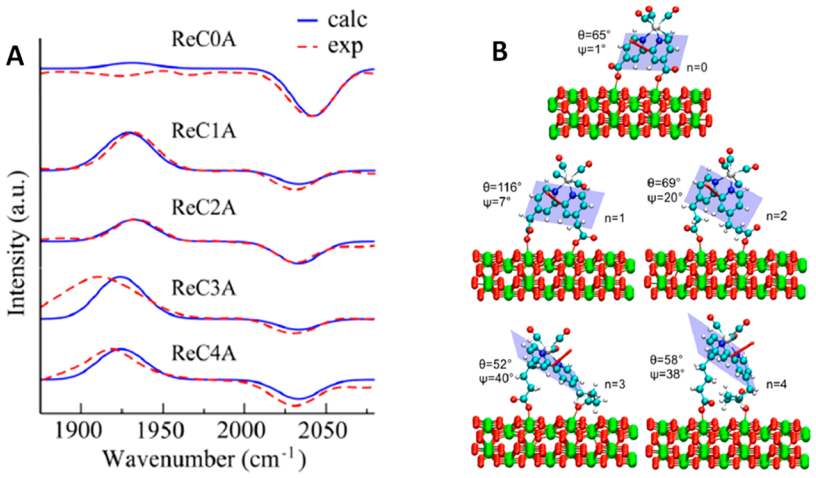

Figure 3. Combined SFG and DFT study of the orientation of ReC*n*A on the rutile TiO_2(001) surface. (A) Comparison of the imaginary parts of the measured (dashed curves) and simulated (solid curves) SFG spectra for ReC*n*A complexes. Each simulated spectrum reveals the average orientation angles (θ, ψ) that best fit the experimental spectrum. (B) Optimized binding geometry of ReC*n*A, with orientation angles close to the values calculated from the PS-SFG spectra. Adapted from ref 22. Copyright 2012 American Chemical Society.

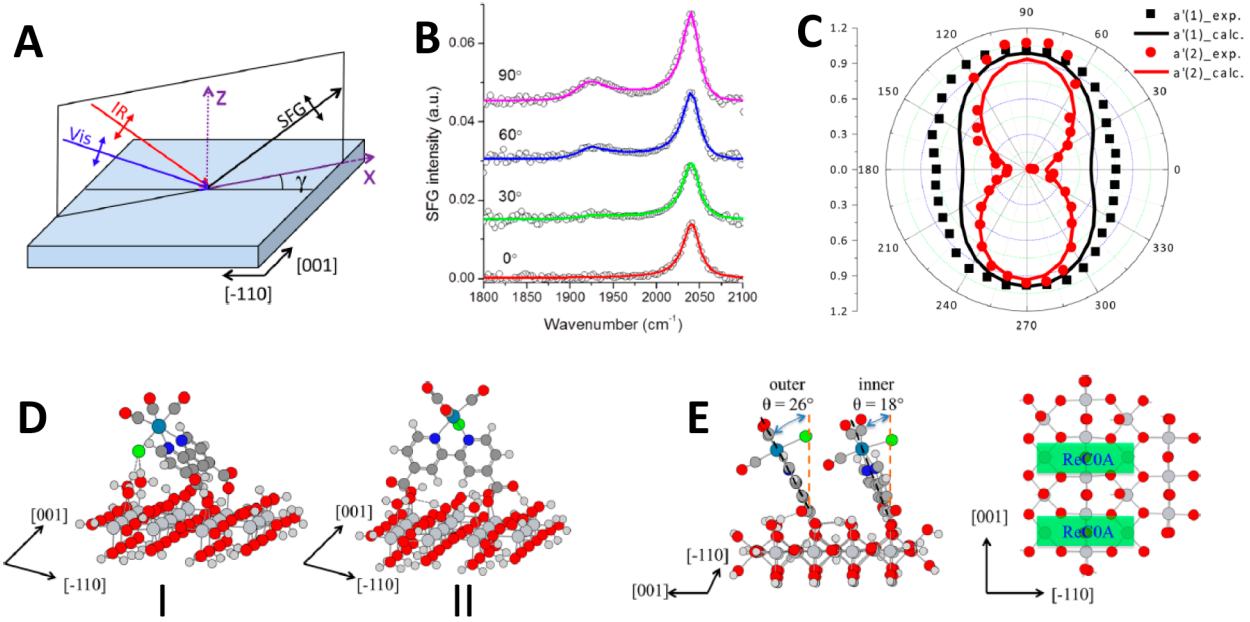

Figure 4. Combined SFG and DFT study of ReC0A on the rutile TiO_2(110) surface. (A) Scheme of the SFG measurement with the *ppp* polarization combination, where γ is the azimuthal angle. (B) SFG spectra of ReC0A/TiO_2(110) at different γ. (C) Experimental and theoretical azimuthal-angle-dependent amplitudes of the a′(1) and a′(2) modes of ReC0A on TiO_2(110). (D) Binding geometry of ReC0A on (110) along the [001] axis (**I**) and the [$\bar{1}$10] axis (**II**). (E) Optimized dimer structure of ReC0A on the (110) surface. Adapted from ref 24. Copyright 2016 American Chemical Society.

studied ReC0A adsorbed on the rutile TiO_2(110) surface, which has C_2 symmetry.[24] Quantitative analysis of the azimuthally dependent SFG responses can reveal the molecular orientation on single-crystalline surfaces (Figure 4A,B).[46,47] Our SFG results support that ReC0A molecules are anisotropically arranged on the TiO_2(110) surface, as is evident from the asymmetric polar plot obtained for the a′(1) and a′(2) stretching modes (Figure 4C). DFT calculations indicate that the binding structure of ReC0A is strongly affected by the TiO_2 atomic arrangement and water on the (110) surface. The structure with ReC0A binding along the [$\bar{1}$10] axis is found to be energetically more favored than that along the [001] axis because of hydrogen bonding between the COOH group and the nearest OH group (Figure 4D). Interestingly, we found that a dimer structure of the catalyst rather than a monomer structure matches the experimental SFG anisotropy trends (Figure 4C,E), suggesting that Re catalysts may form aggregates on the TiO_2(110) surface, similar to those observed for Re catalysts adsorbed on TiO_2 nanoparticles.[16,18] The significantly different surface arrangements of ReC0A on the (001) and (110) surfaces indicate that the molecular binding geometry can be controlled through careful selection of the substrate.

3.2. Re Catalysts on Doped $SrTiO_3$(100)

Photoelectrochemical reduction of CO_2 by the combination of a Re catalyst and a doped semiconductor electrode has been demonstrated.[48] In this regard, the understanding of the effect

DOI: 10.1021/acs.accounts.9b00001
Acc. Chem. Res. 2019, 52, 1289−1300

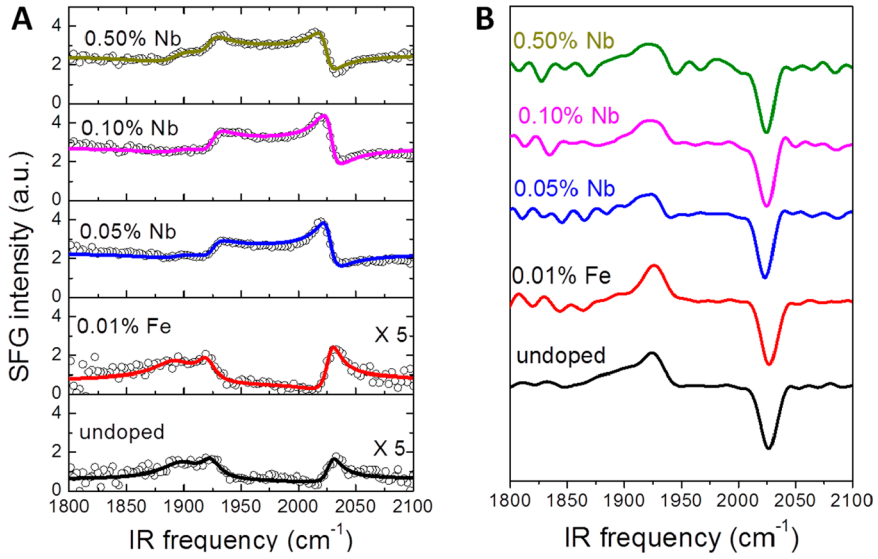

Figure 5. SFG study of ReC0A on the doped $SrTiO_3$ single-crystal (100) surface. (A) Comparison of measured (open circles) and simulated (solid curves) SFG spectra of ReC0A adsorbed on doped $SrTiO_3$(100) surfaces with indicated dopants and dopant concentrations. The spectra of samples on undoped and Fe-doped $SrTiO_3$ are scaled by 5. The fits are based on the Lorentzian model of eq 1. (B) Imaginary spectra of ReC0A adsorbed on different $SrTiO_3$ surfaces. These spectra have been normalized to have the same intensity of the a′(1) mode and displaced vertically for clarity. Adapted from ref 35. Copyright 2018 American Chemical Society.

of doping on the adsorbate−substrate interaction could help in the design of a heterogenized molecular catalyst system used for photoreduction of CO_2. Motivated by this premise, we studied the effect of the doping level in a semiconductor on the molecular structure of an adsorbed Re catalyst. We chose the TiO_2-terminated $SrTiO_3$(100) single-crystal surface as a model system since its surface structure is well-defined.[35] Quite remarkably, both the SFG intensity and the spectral shape for the adsorbed ReC0A show a strong dependence on the doping type and dopant concentration (Figure 5A). The SFG spectra of ReC0A/Nb-doped $SrTiO_3$ show much higher intensity and almost reversed spectral shape compared with those of ReC0A on either undoped or Fe-doped $SrTiO_3$. From a fit of the experimental result to the Lorentzian (eq 1), the difference can be attributed to the stronger magnitude and different phase of the SFG response from the Nb-doped $SrTiO_3$ rather than to an orientation change of the Re catalysts. These results were confirmed by PS-SFG spectroscopy, which showed that all of the spectra have similar features regardless of the dopant level (Figure 5B), indicating similar catalyst binding geometries. To understand the dependence of the SFG responses on the doping level, DFT calculations were performed. The DFT results showed that Nb doping populates the conduction band of $SrTiO_3$, which gives metallic properties to the otherwise insulating $SrTiO_3$. The change in the electronic properties of the n-doped $SrTiO_3$ results in a large nonresonant SFG intensity that interferes with the SFG signals from ReC0A. These results are significant since they indicate that a molecular probe with a well-defined structure can be used to probe the electronic properties of the underlying substrates, and they pave the way for in situ vibrational spectroscopy studies of the photoeletrochemical reaction of heterogenized molecular catalysts on photoelectrodes.

3.3. ReCN and RediCN on Au

Because of the importance of metal interfaces for electrocatalytic reduction of CO_2 in both heterogeneous[49,50] and homogeneous[2,51] systems, it is important to understand the interfacial binding geometry of catalysts, as the orientation can greatly affect electron transfer and substrate access to the active site.[52] As a first effort to develop an effective strategy for anchoring Re complexes to metal electrodes, we investigated the binding geometries of two Re electrocatalysts, Re(R-2,2′-bipyridine)$(CO)_3Cl$ (R = 4-cyano, ReCN; R = 4,4′-dicyano, RediCN), covalently bound on Au surfaces.[23] Quite interestingly, no current response for either immobilized catalyst was observed in aqueous or organic solvents, most likely because of the high overpotential of the complexes, which led to dissociation of the adsorbed complexes from the Au surface before any redox features could be observed. Under no applied potential, however, the complexes were adsorbed onto the surface, as determined by SFG. In Figure 6A,B we present the SFG spectra of ReCN and RediCN, respectively, on gold, which are characterized by a strong nonresonant contribution of the gold. To determinate the geometry of the complex under these conditions, DFT calculations and ab initio SFG simulations of these catalysts on the (111) gold model surface were performed (Figure 6C,D). The simulated SFG spectra from the optimized structures (Figure 6C,D) compare well with the experimental results and confirm that for both complexes the bipyridine ligand is almost parallel to the surface with the axial CO ligand near the surface. The similar binding geometries of the two catalysts suggest that only one cyano group is bonded to the Au surface. Although these catalyst monolayers on the Au surface are not stable at high negative potentials, this work demonstrates the capabilities of our approach of combined SFG spectroscopy and theoretical modeling to determine catalyst structures on electrode surfaces.

4. VIBRATIONAL RELAXATION DYNAMICS OF SURFACE-IMMOBILIZED RE CATALYSTS

The coordination of adsorbates to solid substrates often affects the rates and mechanisms of energy and charge transfer and thus the relative stability of catalytic intermediates.[53−55] Therefore, detailed studies of those fundamental processes

DOI: 10.1021/acs.accounts.9b00001
Acc. Chem. Res. 2019, 52, 1289−1300

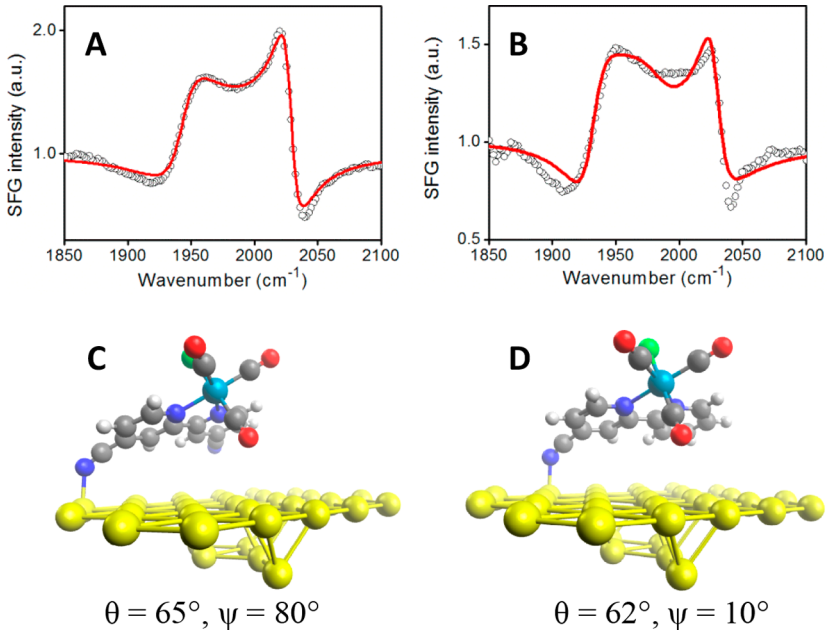

Figure 6. ReCN and RediCN on Au electrodes. (A, B) SFG spectra of (A) RediCN and (B) ReCN SAMs adsorbed on Au thin films (black circles). Red lines are ab initio-simulated SFG spectra. (C, D) DFT-optimized monodentate geometries for RediCN and ReCN, respectively. Values indicated are the tilt angle (θ) and twist angle (ψ) of the bypiridine ring with respect to the normal. Adapted from ref 23. Copyright 2016 American Chemical Society.

on both semiconductor and metal surfaces are essential to gain insights into the reaction dynamics of both photo- and electrocatalytic systems. To this end, TR-SFG spectroscopy (Figure 1B) provides a unique technique with surface specificity and time resolution to investigate energy transfer processes in the heterogenized molecular catalyst systems. To explore the interfacial dynamics of adsorbed catalysts, we have employed TR-SFG spectroscopy to examine the ultrafast vibrational relaxation dynamics of Re catalysts adsorbed on TiO_2 and Au surfaces.[27,28,30]

As discussed in the previous section, the molecular binding structure of Re catalyst is affected by the crystallographic facet of the underlying TiO_2 substrate. An interesting natural question that arises from these findings is whether the crystallographic facet or the molecular structure can also influence the energy transfer process. We chose ReC0A on TiO_2(110) as a model system to study the energy transfer process of the Re catalyst on the semiconductor surface. The IR pump−SFG probe transient measurements show that the population decay of the excited CO stretching modes consists of an ultrafast initial component, associated with rapid equilibration of populations among the three CO stretching modes, and a longer-time-scale T_1 (tens of picoseconds) in which recovery of the ground vibrational state is obtained.[28] In comparison with that of ReC0A on a TiO_2 nanoporous film, the vibrational relaxation time T_1 of ReC0A on TiO_2(110) turns out to be slightly longer, which may suggest a dependence on the crystal facet. Petersen and co-workers recently reported that T_1 of ReC0A is dependent on the crystallographic facet, as observed by TR-SFG of ReC0A on the (001) and (110) surfaces of rutile TiO_2.[29] The latter was found to have a longer lifetime than the former, indicating different couplings between the adsorbate and substrate. Two-dimensional (2D) SFG measurements by the same group also revealed structural heterogeneity of ReC0A monolayers on a TiO_2 nanostructured film.[26,56]

Since electron−hole pair (EHP) excitation is known to influence the chemical dynamics of small molecules such as carbon monoxide adsorbed on metal surfaces,[57] it is crucial to examine whether the energy transfer dynamics of the Re catalyst can be influenced by the same process. To this end, we used TR-SFG spectroscopy to investigate the vibrational relaxation dynamics of RediCN self-assembled on Au.[30] This system was chosen because the RediCN molecule was found to absorb on gold with its bipyridine ligand quite parallel to the surface and axial CO close to the surface (Figure 6C,D).[23] Similar to the ReC0A/TiO_2 system, the kinetics of the CO stretching mode vibrational relaxation of RediCN/Au exhibits a biexponential decay (Figure 7A,B). The kinetics of the a′(1) mode can be modeled as a fast component ($\tau_{\nu-\nu} \approx 2$ ps) and a slow component ($T_1 = 25 \pm 2$ ps), surprisingly similar to analogous measurements in polar aprotic solvents that have no high-frequency modes in resonance with the carbonyl stretching modes.[30] For the same catalyst system, Xiong and co-workers also performed multidimensional SFG measurements exploring the Re catalyst−Au interactions and the interstate coherent dynamics and found that the surface can introduce new homogeneous dephasing pathways.[58,59]

To further elucidate the energy transfer mechanism of RediCN on Au, we performed a combination study of DFT, ab initio molecular dynamics, and time-dependent perturbation theory to calculate intramolecular vibrational relaxation times and EHP coupling on Au. We found that the a′(2) mode (Figure 7C) exhibits the shortest vibrational lifetime since in this normal mode the axial carbonyl group interacts closely with the surface. Therefore, that mode is the primary channel for energy transfer by excitation of EHPs in the Au slab, which has the same time scale as IVR. Additional pathways of energy deactivation, such as phonon-induced relaxation, can be ruled out by comparing the nearly identical kinetics of ReC0A tethered to Au through a long alkanethiol linker (ReC0-Au, Scheme 1) and ReC0A in DMF.[27] These results have direct

DOI: 10.1021/acs.accounts.9b00001
Acc. Chem. Res. 2019, 52, 1289−1300

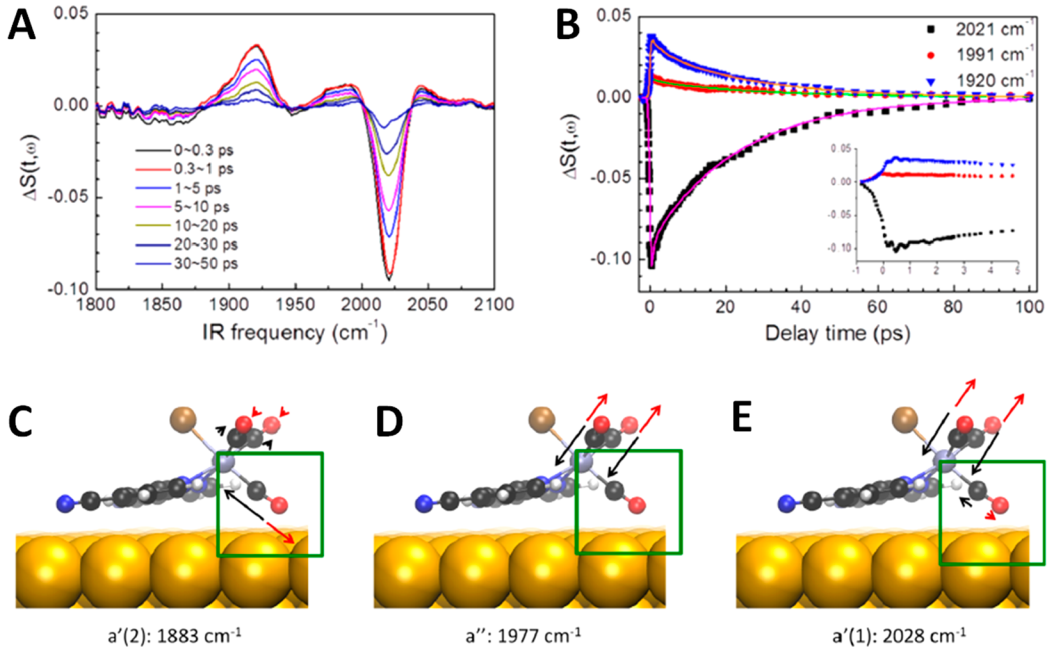

Figure 7. Vibrational relaxation dynamics of RediCN on Au. (A) TR-SFG difference spectra of a RediCN SAM on a Au surface at different delay times. (B) Kinetics at 2021 cm^{-1} (ground-state bleach/stimulated emission for the a′(1) mode), 1991 cm^{-1} (excited-state absorption for the a′(1) mode), and 1920 cm^{-1} (ground-state bleach/stimulated emission for low-frequency modes). Symbols represent experimental data; solid curves represent kinetic fits. (C−E) CO stretching modes of RediCN on the Au surface. Black and red arrows show atomic displacements for C and O, respectively. Green squares highlight the axial CO, and the ab initio frequencies are given underneath. Adapted from ref 30. Copyright 2017 American Chemical Society.

implications for catalytic functionality because EHP-induced vibrational relaxation often alters the reaction mechanism of adsorbed catalysts and might allow for additional control of catalysis via light-driven EHP enhancement.[60,61]

5. ELECTRIC FIELD STRENGTH EXPERIENCED BY SURFACE-IMMOBILIZED MOLECULAR CATALYSTS

Interfacial electric fields have been known to affect many heterogeneous catalytic reactions[62] by increasing reaction rates,[63] controlling selectivity,[64] and increasing reagent concentration.[65] Moreover, in enzymatic systems, the strong local electric fields at the active sites are known to facilitate the catalytic reaction through stabilization of the intermediates.[66] Thus, elucidating how the strong electric fields at the electrolyte−electrode interface can modulate the catalytic process of molecular catalysts is of critical importance and an active area of research. A well-known method to probe the local electric field of molecular systems is the vibrational Stark effect,[67,68] which is based on the fact that the vibrational energy levels of a probe are (de)stabilized differently by an applied electric field, and therefore, the applied electric field will induce a frequency shift of the transition. The relation between the vibrational frequency and the applied electric field is given (to first order in the electric field) by[68]

$$\omega(\phi) = \omega_0 - \Delta\boldsymbol{\mu}\cdot\mathbf{F}(\phi) \tag{3}$$

where ω_0 is the frequency without the local electric field, $\mathbf{F}(\phi)$ is the potential-dependent local electric field, and $\Delta\boldsymbol{\mu}$ is the difference between the dipole moments of the ground and excited vibrational modes. In the previous equation, we have made explicit the dependence of the electric field on the applied voltage of the electrochemical cell, ϕ, which is the experimental controllable parameter. Hence, from measurements of the applied-bias-dependent frequency $\omega(\phi)$ and the value of $\Delta\boldsymbol{\mu}$ obtained from theoretical calculations or experimental measurements, the interfacial electric field strength can be quantified.

As a first step in the direction of understanding the effect of the interfacial electric field on the activity of catalysts in operando, we examined the local electric field at the catalytically active metal center of Re(4-mercapto-2,2-bipyridine)$(CO)_3Cl$ (ReS) and Mn(4-mercapto-2,2-bipyridine)$(CO)_3Cl$ (MnS) SAMs bound on Au surfaces by measuring the Stark tuning of the CO stretching modes by electrochemical SFG spectroscopy (Figure 1D) and DFT calculations.[25] Figure 8A shows the SFG spectra of a SAM of ReS catalyst on a Au electrode in the potential range of −1.3 to 0.3 V. Both the frequency and amplitude of the CO stretching modes as well as the nonresonant SFG signal strongly depend on the applied potential. The symmetric contour plot between the anodic and cathodic sweeps of the potential demonstrates that the monolayers undergo a reversible process. The best linear fit of the frequency shift of the a′(1) mode between 0 and −1.0 V, where no catalytic evolution is observed, gives a Stark tuning slope $d\omega(\phi)/d\phi$ of ∼20.8 cm^{-1}/V (Figure 8B). Additionally, the magnitude of the nonresonant signal presents a minimum at ca. −0.2 V (Figure 8C), which can be assigned to the potential of zero charge (PZC) of the Au/SAM/electrolyte system, a potential at which the contribution of the interfacial-electric-field-induced SFG signal is at a minimum.[69] The Stark tuning rates $\Delta\boldsymbol{\mu}$ for both catalysts on gold surfaces were determined using DFT calculations by computing the frequency-field dependence in the presence of a uniform electric field perpendicular to the surface. We found that the gold surface strongly modulates the Stark tuning rate for configurations with the CO motifs facing the surface, akin to the modulation of the vibrational energy relaxation observed in

DOI: 10.1021/acs.accounts.9b00001
Acc. Chem. Res. 2019, 52, 1289−1300

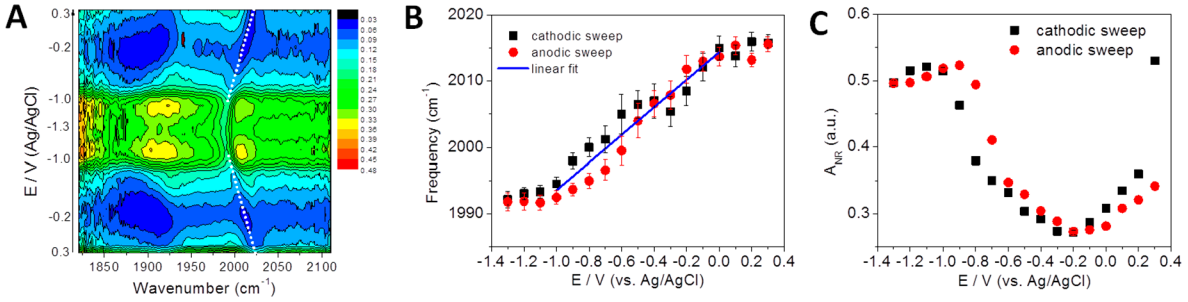

Figure 8. (A) Potential-dependent SFG spectra of the ReS SAM on polycrystalline Au measured over the potential range of 0.3 to −1.3 V (vs Ag/AgCl, 3 M NaCl). A 10 mM KOH aqueous solution was used as the electrolyte. Dashed white lines indicate the shift in the a′(1) stretching mode. (B) Stark tuning of the a′(1) stretching mode of ReS. The blue line is a linear fit. (C) Potential-dependent nonresonant SFG response of the ReS SAM. Adapted from ref 25. Copyright 2018 American Chemical Society.

the previous section.[30] Combining the DFT and the experimental data shows that the electric field strength at the active sites of both the Re and Mn complexes is on the order of 10^8−10^9 V/m, in agreement with previous studies on molecular or ionic systems.[32,33,70−72] It is noteworthy that the magnitude of the electric field experienced by ReS and MnS is similar to that of catalytically active sites of enzymes, suggesting that electric effects similar to the ones found in biological systems might occur in the electrocatalytic systems.[66] Unfortunately, no catalytic activity was examined in this study because the catalyst desorbs at potentials more negative than −1.0 V. This work suggests that with the development of new anchoring strategies to stabilize the catalysts at negative potentials, in situ electrochemical SFG may enable studies of the effects of the electric field on the reaction mechanism of surface-immobilized molecular catalysts.

6. SUMMARY AND PERSPECTIVES

Surface-immobilized molecular catalysts represent a promising approach for the rational development of efficient photocatalytic and electrocatalytic materials. However, in order to achieve robust, efficient, and stable heterogenized molecular catalysts, it is essential to understand their fundamental physicochemical properties, such as surface-bound structures, substrate−adsorbate interactions, and photoinduced or electric-field-induced effects on the catalysts. In this Account, we have summarized our recent combined SFG spectroscopy, theoretical modeling, and synthetic chemistry studies of Re bipyridyl tricarbonyl molecular CO_2 reduction catalysts with various anchoring groups immobilized on semiconductor and metal surfaces. We have focused mainly on three aspects of the heterogenized molecular catalysts: (1) interfacial molecular geometry, (2) interfacial energy transfer, and (3) interfacial electric fields. Our results show that the binding structure of Re catalysts can be significantly influenced by the crystallographic facet of the surface as well as the nature and length of the anchoring group, demonstrating that a particular orientation of the complex can be achieved by a carefully tailored synthetic design. Moreover, since different binding geometries can modulate adsorbate−substrate interactions, the mechanisms of energy and charge transfer can be modulated, as is evident from the influence on the vibrational relaxation dynamics of the Re catalyst due to the crystallographic facet of the substrate or electron−hole pair excitations on gold. In a step toward understanding the effect of the electric field on the activity of catalysts, we also performed an in situ electrochemical SFG study of Re and Mn catalysts adsorbed on Au, which revealed that the catalysts experience electric fields of ca. 10^8−10^9 V/m.

The work presented here demonstrates that SFG is a powerful probe of the molecular structure and dynamics of adsorbed molecular catalysts. However, to tap the huge potential of SFG as a molecular probe of photo- and electrocatalytic processes at interfaces, a few shortcomings need to be overcome. For example, SFG signals from molecular catalyst SAMs adsorbed on semiconductor single-crystal surfaces are usually too weak for time-resolved measurements with optical excitation. The development of a high-repetition-rate SFG system[73] will be beneficial to enhance the sensitivity of TR-SFG measurements, providing insight into photoinduced dynamics processes, including charge transfer, redox reactions, and the mechanism of photocatalytic CO_2 reduction. On the other hand, in operando SFG measurements are still challenging because of the strong IR absorption from the solvent in the electrolyte layer (Figure 1D).[31] The development of an electrode that is transparent in both the IR and visible regions,[74] which allows internal reflection measurements or novel SFG schemes, should be helpful to overcome such problems and allow flexible integration of many electrode materials.[9,17] The integration of 2D SFG spectroscopy, a powerful technique for investigating structure heterogeneity and dynamics, vibrational relaxation, and equilibrium exchange dynamics,[26,56,58,75−77] with electrochemical measurements can provide further structural and dynamical insights on immobilized molecular catalysts. Finally, in situ SFG microscopy with high spatial resolution may enable probing of the effects of heterogeneity of the substrate on the binding configurations and reaction dynamics of molecular catalysts.[78]

AUTHOR INFORMATION

Corresponding Authors

*V.S.B.: victor.batista@yale.edu.
*T.L.: tlian@emory.edu.
*C.P.K.: ckubiak@ucsd.edu.

ORCID

Aimin Ge: 0000-0003-0127-3193
Benjamin Rudshteyn: 0000-0002-9511-6780
Pablo E. Videla: 0000-0003-0742-0342
Clifford P. Kubiak: 0000-0003-2186-488X
Victor S. Batista: 0000-0002-3262-1237
Tianquan Lian: 0000-0002-8351-3690

DOI: 10.1021/acs.accounts.9b00001
Acc. Chem. Res. 2019, 52, 1289−1300

Author Contributions

[‖]A.G., B.R., and P.E.V. contributed equally.

Notes

The authors declare no competing financial interest.

Biographies

Aimin Ge received his B.S. in Chemical Physics from the University of Science and Technology of China in 2008 and his Ph.D. in Environmental Sciences from Hokkaido University in 2014. He is currently a postdoctoral researcher at Emory University. His research interests involve the use of vibrational spectroscopies to study catalytic reactions and ultrafast dynamics at electrode surfaces.

Benjamin Rudshteyn received his B.S. in Chemistry from the Macaulay Honors College at Brooklyn College of the City University of New York in 2013 and earned his Ph.D. from Yale University in 2018. He is currently a postdoctoral researcher at Columbia University. His research interests involve the use of computational chemistry toward the understanding and design of better catalysts.

Pablo E. Videla received his *Licenciatura en Ciencias Química* in 2011 and Ph.D. in Chemistry in 2015 from the University of Buenos Aires. He is currently a postdoctoral researcher at Yale University. His research interests are focused on the use of quantum-mechanical and semiclassical methods to understand the dynamics of complex systems as well as the use of path-integral-based methodologies to study the influence of nuclear quantum effects.

Christopher J. Miller received his B.S. in chemistry from Colorado State University in 2016. He is currently a graduate student at the University of California, San Diego. His research interests involve the synthesis, characterization, and electrochemical study of surface-attached CO_2 reduction catalysts.

Clifford P. Kubiak received his B.S. from Brown University in 1975 and Ph.D. from the University of Rochester in 1980. He was a postdoctoral associate at the Massachusetts Institute of Technology in 1980−1981 and then went on to become a faculty member at Purdue University from 1982 to 1998. He moved to the University of California, San Diego as the Harold C. Urey Endowed Chair Professor in 1998. His research interests include ultrafast electron transfer, homogeneous reduction of CO_2 to liquid fuels, and attachment of CO_2 reduction catalysts to electrode surfaces.

Victor S. Batista received his B.S. from the University of Buenos Aires in 1989 and his Ph.D. from Boston University in 1996. He was a postdoctoral fellow at the University of California at Berkeley (1997−1999) and the University of Toronto (2000−2001). He is currently a Professor in the Department of Chemistry at Yale University. His research interests are focused on the use of semiclassical and quantum-mechanical methods to understand excited-state reaction dynamics, electron transfer, relaxation phenomena, and ligand binding interactions in complicated systems.

Tianquan (Tim) Lian received his B.S. from Xiamen University in 1985, his M.S. from the Chinese Academy of Sciences in 1988, his Ph.D. from the University of Pennsylvania in 1993, and postdoctoral training at the University of California, Berkeley (1994−1996). He is currently the William Henry Emerson Professor in the Department of Chemistry at Emory University. His research interests are focused on understanding the fundamental physical chemistry problems of interfaces, nanomaterials, and solar energy conversion.

■ ACKNOWLEDGMENTS

Early work was supported by DOE BES (DE-FG02-07ER15909 (V.S.B.) and DE-FG02-07ER-15906 (T.L.)). More recent work was supported by the AFOSR (FA9550-13-1-0020 and FA9550-17-0198 (V.S.B., T.L., and C.P.K.)). V.S.B. acknowledges high-performance computing time from NERSC, DOD Copper, and the Yale Center for Research Computing. B.R. gratefully acknowledges support from the NSF Graduate Research Fellowship (DGE-1122492).

■ REFERENCES

(1) Kuramochi, Y.; Ishitani, O.; Ishida, H. Reaction Mechanisms of Catalytic Photochemical CO_2 Reduction Using Re(I) and Ru(II) Complexes. *Coord. Chem. Rev.* **2018**, *373*, 333−356.

(2) Benson, E. E.; Kubiak, C. P.; Sathrum, A. J.; Smieja, J. M. Electrocatalytic and Homogeneous Approaches to Conversion of CO_2 to Liquid Fuels. *Chem. Soc. Rev.* **2009**, *38*, 89−99.

(3) Hawecker, J.; Lehn, J.-M.; Ziessel, R. Electrocatalytic Reduction of Carbon Dioxide Mediated by Re(bipy)$(CO)_3$Cl (Bipy = 2,2-Bipyridine). *J. Chem. Soc., Chem. Commun.* **1984**, 328−330.

(4) Hawecker, J.; Lehn, J. M.; Ziessel, R. Photochemical and Electrochemical Reduction of Carbon Dioxide to Carbon Monoxide Mediated by (2,2′-Bipyridine)Tricarbonylchlororhenium(I) and Related Complexes as Homogeneous Catalysts. *Helv. Chim. Acta* **1986**, *69*, 1990−2012.

(5) Smieja, J. M.; Kubiak, C. P. Re(bipy-tBu)$(CO)_3$Cl-Improved Catalytic Activity for Reduction of Carbon Dioxide: IR-Spectroelectrochemical and Mechanistic Studies. *Inorg. Chem.* **2010**, *49*, 9283−9289.

(6) Won, D.-I.; Lee, J.-S.; Ji, J.-M.; Jung, W.-J.; Son, H.-J.; Pac, C.; Kang, S. O. Highly Robust Hybrid Photocatalyst for Carbon Dioxide Reduction: Tuning and Optimization of Catalytic Activities of Dye/TiO_2/Re(I) Organic−Inorganic Ternary Systems. *J. Am. Chem. Soc.* **2015**, *137*, 13679−13690.

(7) Windle, C. D.; Reisner, E. Heterogenised Molecular Catalysts for the Reduction of CO_2 to Fuels. *Chimia* **2015**, *69*, 435−441.

(8) Windle, C. D.; Pastor, E.; Reynal, A.; Whitwood, A. C.; Vaynzof, Y.; Durrant, J. R.; Perutz, R. N.; Reisner, E. Improving the Photocatalytic Reduction of CO_2 to CO through Immobilisation of a Molecular Re Catalyst on TiO_2. *Chem. - Eur. J.* **2015**, *21*, 3746−3754.

(9) Oh, S.; Gallagher, J. R.; Miller, J. T.; Surendranath, Y. Graphite-Conjugated Rhenium Catalysts for Carbon Dioxide Reduction. *J. Am. Chem. Soc.* **2016**, *138*, 1820−1823.

(10) Schreier, M.; Luo, J.; Gao, P.; Moehl, T.; Mayer, M. T.; Grätzel, M. Covalent Immobilization of a Molecular Catalyst on Cu_2O Photocathodes for CO_2 Reduction. *J. Am. Chem. Soc.* **2016**, *138*, 1938−1946.

(11) Kiefer, L. M.; King, J. T.; Kubarych, K. J. Dynamics of Rhenium Photocatalysts Revealed through Ultrafast Multidimensional Spectroscopy. *Acc. Chem. Res.* **2015**, *48*, 1123−1130.

(12) Asbury, J. B.; Wang, Y.; Lian, T. Time-Dependent Vibration Stokes Shift During Solvation: Experiment and Theory. *Bull. Chem. Soc. Jpn.* **2002**, *75*, 973−983.

(13) Dattelbaum, D. M.; Omberg, K. M.; Schoonover, J. R.; Martin, R. L.; Meyer, T. J. Application of Time-Resolved Infrared Spectroscopy to Electronic Structure in Metal-to-Ligand Charge-Transfer Excited States. *Inorg. Chem.* **2002**, *41*, 6071−6079.

(14) Kraack, J. P.; Hamm, P. Surface-Sensitive and Surface-Specific Ultrafast Two-Dimensional Vibrational Spectroscopy. *Chem. Rev.* **2017**, *117*, 10623−10664.

(15) Rosenfeld, D. E.; Gengeliczki, Z.; Smith, B. J.; Stack, T. D. P.; Fayer, M. D. Structural Dynamics of a Catalytic Monolayer Probed by Ultrafast 2D IR Vibrational Echoes. *Science* **2011**, *334*, 634−639.

(16) Laaser, J. E.; Christianson, J. R.; Oudenhoven, T. A.; Joo, Y.; Gopalan, P.; Schmidt, J. R.; Zanni, M. T. Dye Self-Association Identified by Intermolecular Couplings between Vibrational Modes as Revealed by Infrared Spectroscopy, and Implications for Electron Injection. *J. Phys. Chem. C* **2014**, *118*, 5854−5861.

(17) Reuillard, B.; Ly, K. H.; Rosser, T. E.; Kuehnel, M. F.; Zebger, I.; Reisner, E. Tuning Product Selectivity for Aqueous CO_2 Reduction

DOI: 10.1021/acs.accounts.9b00001
Acc. Chem. Res. 2019, 52, 1289−1300

with a Mn(Bipyridine)-Pyrene Catalyst Immobilized on a Carbon Nanotube Electrode. *J. Am. Chem. Soc.* **2017**, *139*, 14425−14435.
(18) Oudenhoven, T. A.; Joo, Y.; Laaser, J. E.; Gopalan, P.; Zanni, M. T. Dye Aggregation Identified by Vibrational Coupling Using 2D IR Spectroscopy. *J. Chem. Phys.* **2015**, *142*, 212449.
(19) Kraack, J. P.; Frei, A.; Alberto, R.; Hamm, P. Ultrafast Vibrational Energy Transfer in Catalytic Monolayers at Solid-Liquid Interfaces. *J. Phys. Chem. Lett.* **2017**, *8*, 2489−2495.
(20) Paoprasert, P.; Laaser, J. E.; Xiong, W.; Franking, R. A.; Hamers, R. J.; Zanni, M. T.; Schmidt, J. R.; Gopalan, P. Bridge-Dependent Interfacial Electron Transfer from Rhenium-Bipyridine Complexes to TiO_2 Nanocrystalline Thin Films. *J. Phys. Chem. C* **2010**, *114*, 9898−9907.
(21) Shen, Y. *Fundamentals of Sum-Frequency Spectroscopy*; Cambridge University Press, 2016.
(22) Anfuso, C. L.; Xiao, D.; Ricks, A. M.; Negre, C. F.; Batista, V. S.; Lian, T. Orientation of a Series of CO_2 Reduction Catalysts on Single Crystal TiO_2 Probed by Phase-Sensitive Vibrational Sum Frequency Generation Spectroscopy (PS-VSFG). *J. Phys. Chem. C* **2012**, *116*, 24107−24114.
(23) Clark, M. L.; Rudshteyn, B.; Ge, A.; Chabolla, S. A.; Machan, C. W.; Psciuk, B. T.; Song, J.; Canzi, G.; Lian, T.; Batista, V. S.; Kubiak, C. P. Orientation of Cyano-Substituted Bipyridine Re(I) *fac*-Tricarbonyl Electrocatalysts Bound to Conducting Au Surfaces. *J. Phys. Chem. C* **2016**, *120*, 1657−1665.
(24) Ge, A.; Rudshteyn, B.; Psciuk, B. T.; Xiao, D.; Song, J.; Anfuso, C. L.; Ricks, A. M.; Batista, V. S.; Lian, T. Surface-Induced Anisotropic Binding of a Rhenium CO_2-Reduction Catalyst on Rutile TiO_2(110) Surfaces. *J. Phys. Chem. C* **2016**, *120*, 20970−20977.
(25) Clark, M. L.; Ge, A.; Videla, P. E.; Rudshteyn, B.; Miller, C. J.; Song, J.; Batista, V. S.; Lian, T.; Kubiak, C. P. CO_2 Reduction Catalysts on Gold Electrode Surfaces Influenced by Large Electric Fields. *J. Am. Chem. Soc.* **2018**, *140*, 17643−17655.
(26) Vanselous, H.; Videla, P. E.; Batista, V. S.; Petersen, P. B. Distinct Binding of Rhenium Catalysts on Nanostructured and Single Crystalline TiO_2 Surfaces Revealed by 2D SFG Spectroscopy. *J. Phys. Chem. C* **2018**, *122*, 26018−26031.
(27) Anfuso, C. L.; Ricks, A. M.; Rodriguez-Cordoba, W.; Lian, T. Q. Ultrafast Vibrational Relaxation Dynamics of a Rhenium Bipyridyl CO_2-Reduction Catalyst at a Au Electrode Surface Probed by Time-Resolved Vibrational Sum Frequency Generation Spectroscopy. *J. Phys. Chem. C* **2012**, *116*, 26377−26384.
(28) Ricks, A. M.; Anfuso, C. L.; Rodriguez-Cordoba, W.; Lian, T. Vibrational Relaxation Dynamics of Catalysts on TiO_2 Rutile (110) Single Crystal Surfaces and Anatase Nanoporous Thin Films. *Chem. Phys.* **2013**, *422*, 264−271.
(29) Calabrese, C.; Vanselous, H.; Petersen, P. B. Deconstructing the Heterogeneity of Surface-Bound Catalysts: Rutile Surface Structure Affects Molecular Properties. *J. Phys. Chem. C* **2016**, *120*, 1515−1522.
(30) Ge, A.; Rudshteyn, B.; Zhu, J.; Maurer, R. J.; Batista, V. S.; Lian, T. Electron-Hole-Pair-Induced Vibrational Energy Relaxation of Rhenium Catalysts on Gold Surfaces. *J. Phys. Chem. Lett.* **2018**, *9*, 406−412.
(31) Neri, G.; Walsh, J. J.; Teobaldi, G.; Donaldson, P. M.; Cowan, A. J. Detection of Catalytic Intermediates at an Electrode Surface During Carbon Dioxide Reduction by an Earth-Abundant Catalyst. *Nat. Catal.* **2018**, *1*, 952−959.
(32) Patrow, J. G.; Sorenson, S. A.; Dawlaty, J. M. Direct Spectroscopic Measurement of Interfacial Electric Fields near an Electrode under Polarizing or Current-Carrying Conditions. *J. Phys. Chem. C* **2017**, *121*, 11585−11592.
(33) Ge, A.; Videla, P. E.; Lee, G. L.; Rudshteyn, B.; Song, J.; Kubiak, C. P.; Batista, V. S.; Lian, T. Interfacial Structure and Electric Field Probed by in Situ Electrochemical Vibrational Stark Effect Spectroscopy and Computational Modeling. *J. Phys. Chem. C* **2017**, *121*, 18674−18682.
(34) Anfuso, C. L.; Snoeberger, R. C.; Ricks, A. M.; Liu, W.; Xiao, D.; Batista, V. S.; Lian, T. Covalent Attachment of a Rhenium Bipyridyl CO_2 Reduction Catalyst to Rutile TiO_2. *J. Am. Chem. Soc.* **2011**, *133*, 6922−6925.
(35) Ge, A.; Videla, P. E.; Rudshteyn, B.; Liu, Q.; Batista, V. S.; Lian, T. Dopant-Dependent SFG Response of Rhenium CO_2 Reduction Catalysts Chemisorbed on $SrTiO_3$(100) Single Crystals. *J. Phys. Chem. C* **2018**, *122*, 13944−13952.
(36) Song, J.; Ge, A.; Piercy, B.; Losego, M. D.; Lian, T. Effects of Al_2O_3 Atomic Layer Deposition on Interfacial Structure and Electron Transfer Dynamics at Re-Bipyridyl Complex/TiO_2 Interfaces. *Chem. Phys.* **2018**, *512*, 68−74.
(37) Nihonyanagi, S.; Mondal, J. A.; Yamaguchi, S.; Tahara, T. Structure and Dynamics of Interfacial Water Studied by Heterodyne-Detected Vibrational Sum-Frequency Generation. *Annu. Rev. Phys. Chem.* **2013**, *64*, 579−603.
(38) Arnolds, H.; Bonn, M. Ultrafast Surface Vibrational Dynamics. *Surf. Sci. Rep.* **2010**, *65*, 45−66.
(39) Zhuang, X.; Miranda, P.; Kim, D.; Shen, Y. Mapping Molecular Orientation and Conformation at Interfaces by Surface Nonlinear Optics. *Phys. Rev. B: Condens. Matter Mater. Phys.* **1999**, *59*, 12632.
(40) Spitler, M. T.; Parkinson, B. A. Dye Sensitization of Single Crystal Semiconductor Electrodes. *Acc. Chem. Res.* **2009**, *42*, 2017−2029.
(41) Wu, X.; Chen, Z.; Lu, G. Q.; Wang, L. Nanosized Anatase TiO_2 Single Crystals with Tunable Exposed (001) Facets for Enhanced Energy Conversion Efficiency of Dye-Sensitized Solar Cells. *Adv. Funct. Mater.* **2011**, *21*, 4167−4172.
(42) Li, C.; Koenigsmann, C.; Ding, W.; Rudshteyn, B.; Yang, K. R.; Regan, K. P.; Konezny, S. J.; Batista, V. S.; Brudvig, G. W.; Schmuttenmaer, C. A.; Kim, J.-H. Facet-Dependent Photoelectrochemical Performance of TiO_2 Nanostructures: An Experimental and Computational Study. *J. Am. Chem. Soc.* **2015**, *137*, 1520−1529.
(43) Abdellah, M.; El-Zohry, A. M.; Antila, L. J.; Windle, C. D.; Reisner, E.; Hammarström, L. Time-Resolved IR Spectroscopy Reveals a Mechanism with TiO_2 as a Reversible Electron Acceptor in a TiO_2−Re Catalyst System for CO_2 Photoreduction. *J. Am. Chem. Soc.* **2017**, *139*, 1226−1232.
(44) Fujishima, A.; Rao, T. N.; Tryk, D. A. Titanium Dioxide Photocatalysis. *J. Photochem. Photobiol., C* **2000**, *1*, 1−21.
(45) Riplinger, C.; Sampson, M. D.; Ritzmann, A. M.; Kubiak, C. P.; Carter, E. A. Mechanistic Contrasts between Manganese and Rhenium Bipyridine Electrocatalysts for the Reduction of Carbon Dioxide. *J. Am. Chem. Soc.* **2014**, *136*, 16285−16298.
(46) Sung, J.; Waychunas, G. A.; Shen, Y. R. Surface-Induced Anisotropic Orientations of Interfacial Ethanol Molecules at Air/Sapphire$1\bar{1}02$ and Ethanol/Sapphire$1\bar{1}02$ Interfaces. *J. Phys. Chem. Lett.* **2011**, *2*, 1831−1835.
(47) Jang, J. H.; Lydiatt, F.; Lindsay, R.; Baldelli, S. Quantitative Orientation Analysis by Sum Frequency Generation in the Presence of Near-Resonant Background Signal: Acetonitrile on Rutile TiO_2(110). *J. Phys. Chem. A* **2013**, *117*, 6288−6302.
(48) Kumar, B.; Smieja, J. M.; Kubiak, C. P. Photoreduction of CO_2 on p-type Silicon Using $Re(bipy\text{-}Bu^t)(CO)_3Cl$: Photovoltages Exceeding 600 mV for the Selective Reduction of CO_2 to CO. *J. Phys. Chem. C* **2010**, *114*, 14220−14223.
(49) Weng, Z.; Jiang, J.; Wu, Y.; Wu, Z.; Guo, X.; Materna, K. L.; Liu, W.; Batista, V. S.; Brudvig, G. W.; Wang, H. Electrochemical CO_2 Reduction to Hydrocarbons on a Heterogeneous Molecular Cu Catalyst in Aqueous Solution. *J. Am. Chem. Soc.* **2016**, *138*, 8076−8079.
(50) Hori, Y.; Kikuchi, K.; Suzuki, S. Production of CO and CH_4 in Electrochemical Reduction of CO_2 at Metal Electrodes in Aqueous Hydrogencarbonate Solution. *Chem. Lett.* **1985**, *14*, 1695−1698.
(51) Windle, C. D.; Perutz, R. N. Advances in Molecular Photocatalytic and Electrocatalytic CO_2 Reduction. *Coord. Chem. Rev.* **2012**, *256*, 2562−2570.
(52) Prezhdo, O. V.; Duncan, W. R.; Prezhdo, V. V. Dynamics of the Photoexcited Electron at the Chromophore−Semiconductor Interface. *Acc. Chem. Res.* **2008**, *41*, 339−348.

DOI: 10.1021/acs.accounts.9b00001
Acc. Chem. Res. 2019, 52, 1289−1300

(53) Zhdanov, V. P.; Zamaraev, K. I. Vibrational Relaxation of Adsorbed Molecules. Mechanisms and Manifestations in Chemical Reactions on Solid Surfaces. *Catal. Rev.: Sci. Eng.* **1982**, *24*, 373−413.
(54) Houston, P. L.; Merrill, R. P. Gas-Surface Interactions with Vibrationally Excited Molecules. *Chem. Rev.* **1988**, *88*, 657−671.
(55) Gruebele, M.; Wolynes, P. G. Vibrational Energy Flow and Chemical Reactions. *Acc. Chem. Res.* **2004**, *37*, 261−267.
(56) Vanselous, H.; Stingel, A. M.; Petersen, P. B. Interferometric 2D Sum Frequency Generation Spectroscopy Reveals Structural Heterogeneity of Catalytic Monolayers on Transparent Materials. *J. Phys. Chem. Lett.* **2017**, *8*, 825−830.
(57) Tully, J. C. Chemical Dynamics at Metal Surfaces. *Annu. Rev. Phys. Chem.* **2000**, *51*, 153−178.
(58) Wang, J.; Clark, M. L.; Li, Y.; Kaslan, C. L.; Kubiak, C. P.; Xiong, W. Short-Range Catalyst−Surface Interactions Revealed by Heterodyne Two-Dimensional Sum Frequency Generation Spectroscopy. *J. Phys. Chem. Lett.* **2015**, *6*, 4204−4209.
(59) Li, Y.; Wang, J.; Clark, M. L.; Kubiak, C. P.; Xiong, W. Characterizing Interstate Vibrational Coherent Dynamics of Surface Adsorbed Catalysts by Fourth-Order 3D SFG Spectroscopy. *Chem. Phys. Lett.* **2016**, *650*, 1−6.
(60) Christopher, P.; Xin, H.; Linic, S. Visible-Light-Enhanced Catalytic Oxidation Reactions on Plasmonic Silver Nanostructures. *Nat. Chem.* **2011**, *3*, 467.
(61) Park, J. Y.; Kim, S. M.; Lee, H.; Nedrygailov, I. I. Hot-Electron-Mediated Surface Chemistry: Toward Electronic Control of Catalytic Activity. *Acc. Chem. Res.* **2015**, *48*, 2475−2483.
(62) Welborn, V. V.; Ruiz Pestana, L.; Head-Gordon, T. Computational Optimization of Electric Fields for Better Catalysis Design. *Nat. Catal.* **2018**, *1*, 649−655.
(63) Pacchioni, G.; Lomas, J. R.; Illas, F. Electric Field Effects in Heterogeneous Catalysis. *J. Mol. Catal. A: Chem.* **1997**, *119*, 263−273.
(64) Gorin, C. F.; Beh, E. S.; Kanan, M. W. An Electric Field−Induced Change in the Selectivity of a Metal Oxide−Catalyzed Epoxide Rearrangement. *J. Am. Chem. Soc.* **2012**, *134*, 186−189.
(65) Liu, M.; Pang, Y.; Zhang, B.; De Luna, P.; Voznyy, O.; Xu, J.; Zheng, X.; Dinh, C. T.; Fan, F.; Cao, C.; et al. Enhanced Electrocatalytic CO_2 Reduction via Field-Induced Reagent Concentration. *Nature* **2016**, *537*, 382−386.
(66) Fried, S. D.; Boxer, S. G. Electric Fields and Enzyme Catalysis. *Annu. Rev. Biochem.* **2017**, *86*, 387−415.
(67) Lambert, D. K. Vibrational Stark Effect of Adsorbates at Electrochemical Interfaces. *Electrochim. Acta* **1996**, *41*, 623−630.
(68) Fried, S. D.; Boxer, S. G. Measuring Electric Fields and Noncovalent Interactions Using the Vibrational Stark Effect. *Acc. Chem. Res.* **2015**, *48*, 998−1006.
(69) Guyot-Sionnest, P.; Tadjeddine, A.; Liebsch, A. Electronic Distribution and Nonlinear Optical Response at the Metal-Electrolyte Interface. *Phys. Rev. Lett.* **1990**, *64*, 1678.
(70) Baldelli, S. Probing Electric Fields at the Ionic Liquid-Electrode Interface Using Sum Frequency Generation Spectroscopy and Electrochemistry. *J. Phys. Chem. B* **2005**, *109*, 13049−13051.
(71) Braunschweig, B.; Mukherjee, P.; Dlott, D. D.; Wieckowski, A. Real-Time Investigations of Pt(111) Surface Transformations in Sulfuric Acid Solutions. *J. Am. Chem. Soc.* **2010**, *132*, 14036−14038.
(72) Oklejas, V.; Sjostrom, C.; Harris, J. M. SERS Detection of the Vibrational Stark Effect from Nitrile-Terminated SAMs to Probe Electric Fields in the Diffuse Double-Layer. *J. Am. Chem. Soc.* **2002**, *124*, 2408−2409.
(73) Yesudas, F.; Mero, M.; Kneipp, J.; Heiner, Z. Vibrational Sum-Frequency Generation Spectroscopy of Lipid Bilayers at Repetition Rates up to 100 kHz. *J. Chem. Phys.* **2018**, *148*, 104702.
(74) Peng, Q.; Chen, J.; Ji, H.; Morita, A.; Ye, S. Origin of the Overpotential for the Oxygen Evolution Reaction on a Well-Defined Graphene Electrode Probed by in Situ Sum Frequency Generation Vibrational Spectroscopy. *J. Am. Chem. Soc.* **2018**, *140*, 15568−15571.
(75) Zhang, Z.; Piatkowski, L.; Bakker, H. J.; Bonn, M. Ultrafast Vibrational Energy Transfer at the Water/Air Interface Revealed by Two-Dimensional Surface Vibrational Spectroscopy. *Nat. Chem.* **2011**, *3*, 888−893.
(76) Inoue, K.-i.; Nihonyanagi, S.; Singh, P. C.; Yamaguchi, S.; Tahara, T. 2D Heterodyne-Detected Sum Frequency Generation Study on the Ultrafast Vibrational Dynamics of H_2O and HOD Water at Charged Interfaces. *J. Chem. Phys.* **2015**, *142*, 212431.
(77) Xiong, W.; Laaser, J. E.; Mehlenbacher, R. D.; Zanni, M. T. Adding a Dimension to the Infrared Spectra of Interfaces Using Heterodyne Detected 2D Sum-Frequency Generation (HD 2D SFG) Spectroscopy. *Proc. Natl. Acad. Sci. U. S. A.* **2011**, *108*, 20902−20907.
(78) Fang, M.; Baldelli, S. Surface-Induced Heterogeneity Analysis of an Alkanethiol Monolayer on Microcrystalline Copper Surface Using Sum Frequency Generation Imaging Microscopy. *J. Phys. Chem. C* **2017**, *121*, 1591−1601.

DOI: 10.1021/acs.accounts.9b00001
Acc. Chem. Res. 2019, 52, 1289−1300